1 APV6 response at high rates

1.1 Introduction

In the CMS tracker silicon detectors will be exposed to a high rate particle flux. We know from simulations that in worst conditions about an equivalent MIP charge will be delivered on each strip about every 1 μs. These extreme working conditions require that front-end electronics have time constants well suited for their operation.

We describe the measurement performed on a sample of front-end chips, the obtained results and their interpretation in the framework of an analysis circuit model.

1.2 Test bench set-up and measurement results

The arrival of a train of particle signals on the front-end channel input has been simulated on a test bench with a voltage staircase ramp applied to the input, through a serial capacitor C_{ext} as shown in figure 1. A scheme of the measurement apparatus is shown in figure 2 where also the particle signal overposed to the "n-th" ramp step is shown, as seen at a digital scope.

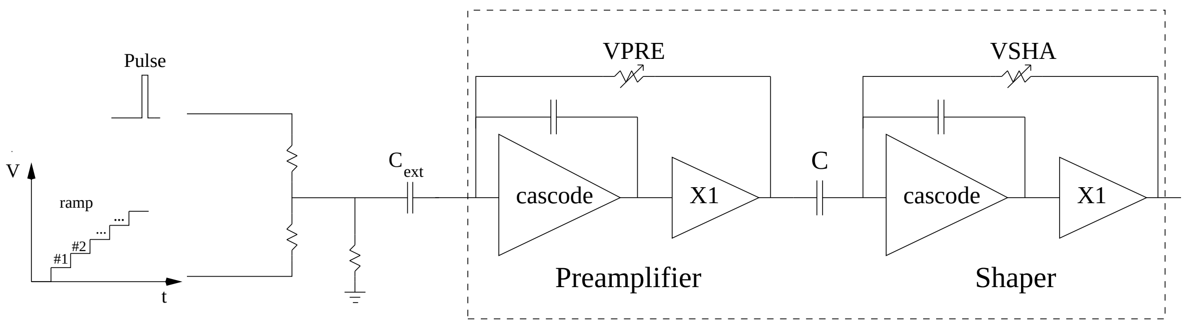

Figure 1: Scheme of front-end channel (shaded rectangle) with the input staircase ramp and the signal pulse.

Height and width of the steps were chosen to simulate respectively the mean charge delivered by particles (MIP) and the mean time between two successive particles. The height pulse was chosen to simulate the MIP peak energy, while its width was set to 200 ns.

Each channel of the front-end chip is based on two similar stages as shown in figure 1. The time constant of the feedback impedance of the first stage (Preamplifier) is usually set at few microseconds or more while the second stage one (Shaper) is set at few tens of nanoseconds in order to obtain a peak time of 50 ns. Time constants can be varied by externally choosing the feedback resistance values.

Typical results are shown in figure 3 where attenuation effects become relevant after about 10 steps and for step width up to 10 μs.

It is clear that the main reason of the observed effect is due to the preamplifier time constant which causes charges accumulation (pile-up), large enough to bring the preamplifier in a marginal working region. This is confirmed by results of figure 4 (full circle points) where the preamplifier time constant was reduced up to cancel the attenuation effect.

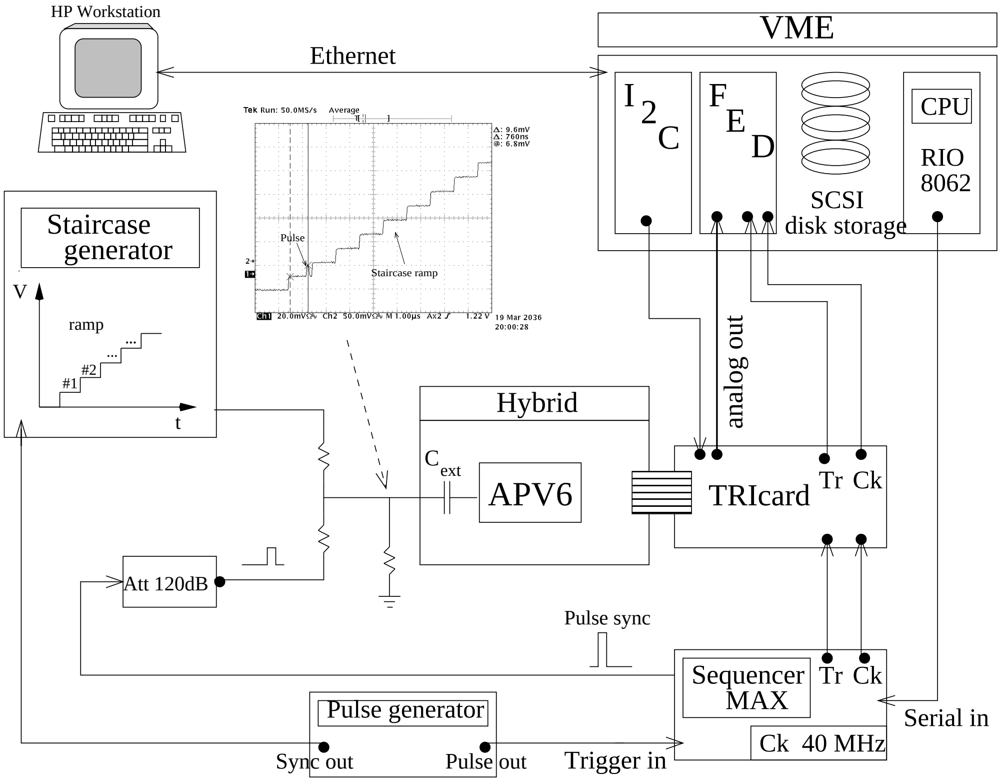

Figure 2: Scheme of the measurements apparatus and staircase ramp with the overposed step pulse at C_{ext} input, as seen at a digital scope.

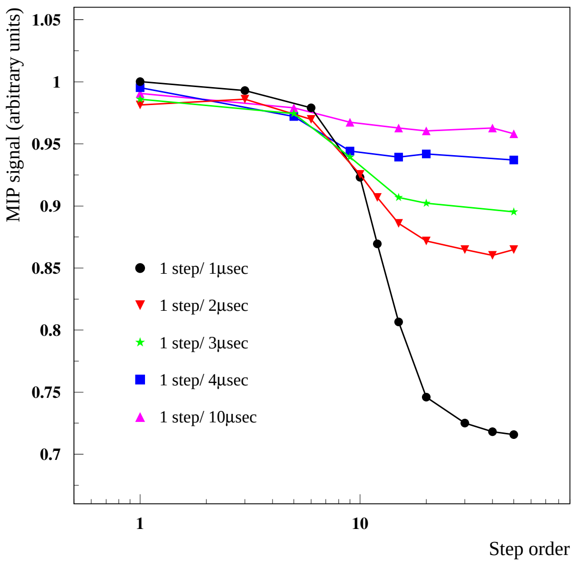

Figure 3: Front-end output (peak value) as a function of the step order as varying the step width from 1μs to 10μs, with standard settings for the APV6 (VSHA=0, VPRE=184).

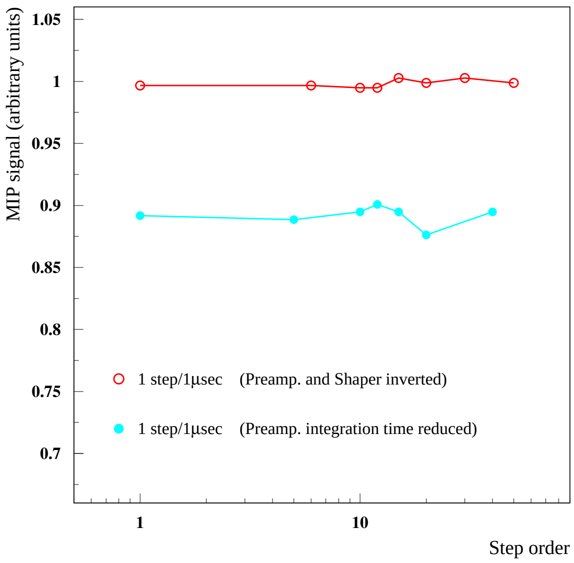

Figure 4: Front-end output (peak value) as a function of the step order, in the case of reduced preamplifier time constant (VSHA=0, VPRE=64) and in the case of preamplifier and shaper inverted time constants (VSHA=184, VPRE=0).

1.3 Shaping at high rates

The reduction of the preamplifier integration time constant eliminates the attenuation effect on the output signal but degrades the output both in shape and in amplitude (figure 5 - square points).

We found that the output shape remains unchanged if we simply swap the preamplifier and the shaper time constants (figure 5, 6 - triangle points). We also verified that in swap mode there is no relevant increase of noise respect to the standard mode (Table 1), expecially in deconvolution mode where the parallel noise contribution is reduced by the small peaking time.

	Peak mode		Deconvolution mode	
	standard mode	swap mode	standard mode	swap mode
σ (ADC counts)	0.91	0.99	1.59	1.60

Table 1: Noise in ADC counts.

Because of the few tens of nanoseconds, typical of the shaper time constant, the input stage of the front-end channel does not suffer anymore of the pile up effect and the output is independent on previous signals even at rates as high as 1 MHz (figure 4 - empty circle points).

The reason of such behavior lies in the symmetry of the circuit with respect to the coupling capacitor C. The following more detailed circuit analysis confirms this simple observation.

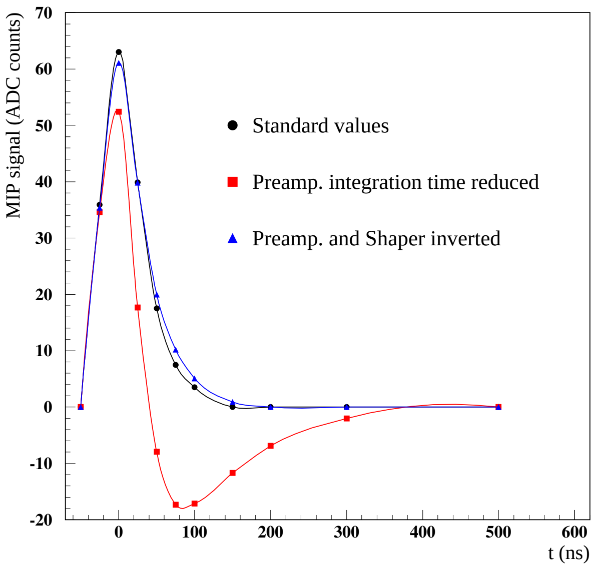

Figure 5: Front-end output shape (in peak mode) for standard values of integration and shaping time constant (●), in the case of reduced integration time constant (■), and in the case of preamplifier and shaper inverted time constants (▲).

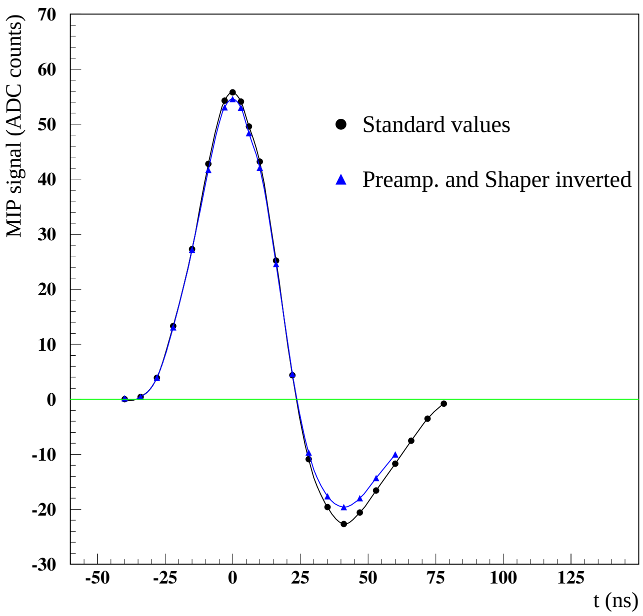

Figure 6: Front-end output shape (in deconvolution mode) for standard values of integration and shaping time constant (●), and in the case of preamplifier and shaper inverted time constants (▲).

SETTINGS	VSHA	VPRE
Standard values	0	184
Preamp. integration time reduced	0	64
Preamp. and Shaper inverted	184	0

Table 2: VSHA and VPRE values for standard settings and swapped ones.

1.4 Circuit analysis of APV6 single front-end channel

In figure 7 the equivalent circuit of one of 128 APV6 front-end channels is shown; both preamplifier and shaper part are based on a cascode with a $C_f = 0.25$ pF feedback; the cascode output, after a source follower, is again fed-back through the feedback transistor channel, whose resistive value can be changed by varying VPRE and VSHA voltage.

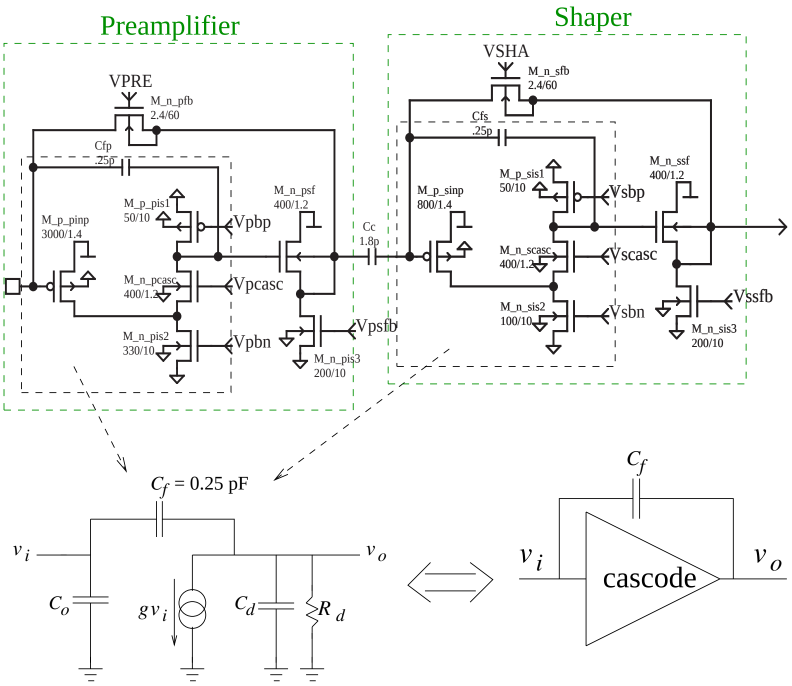

Figure 7: Scheme of APV6 single front-end channel.

This circuit transfer function can be analitically calculated as a function of the input transistor trasconductance and capacitance, the output cascode transistor impedance, the output impedance of the source follower and the preamplifier and shaper feedback resistances.

These unknown quantities can be estimated by fitting the calculated transfer function output to the measured experimental data, in case of a signal particle in input. Fit results are shown in figure 8 for two different APV6 chips and for different VSHA values, and give an integration time constant of about 6 μs.

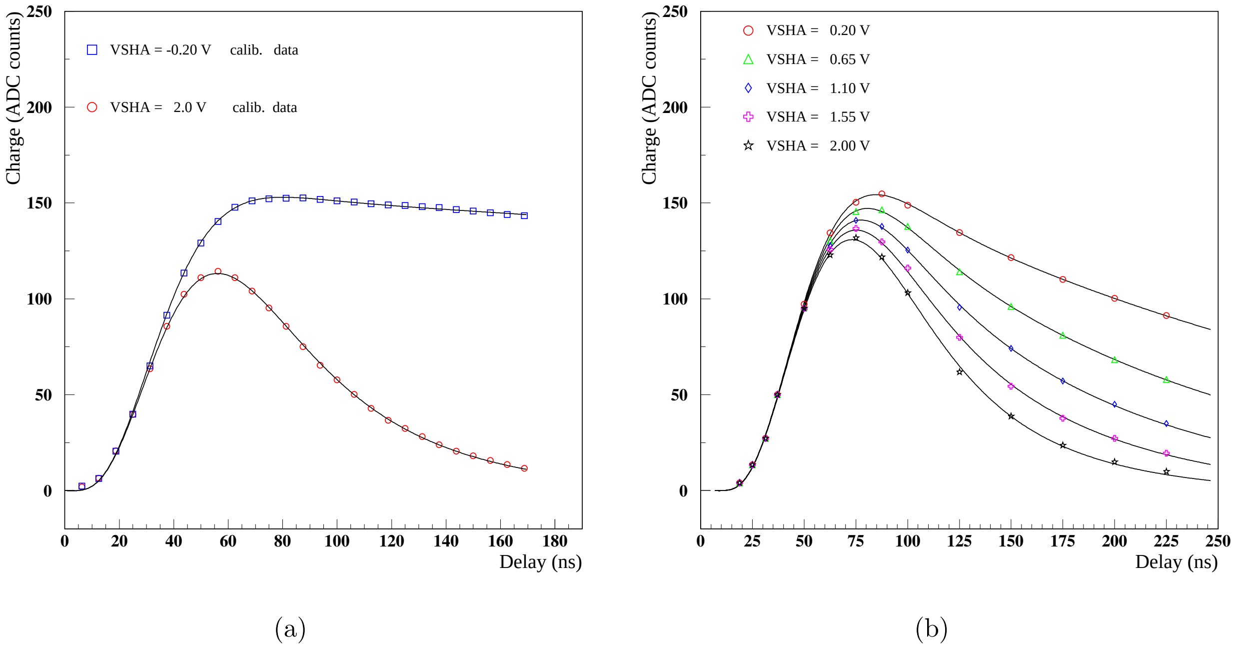

Figure 8: Fit results of the single front-end channel unknown values to experimental measurements of APV6 output.

Once the output shape has been parametrized we have investigated the effects of varying VPRE on signal output. Figure 9 shows our model prediction about the output shape in case of a reduced preamplifier feedback resistance and in case the preamplifier and shaper time constants have been inverted. Such predictions have been confirmed by measurements reported in figure 5.

The aforesaid circuit model allows also to understand why the output shape remains unchanged when the time constants are inverted. In fact we can now estimate the output voltage of the first stage and the input current of the second one before and after the swapping (figure 10).

In case of inverted preamplifier and shaping time constants (figure 10(c)) the first stage acts itself as a shaper with two poles coming from the feedback impedance (with a time constant of few tens of nanoseconds) and the cascode dominant pole. The subsequent coupling capacitor C and the following stage with a time constant of the order of some microseconds act simply as an amplifier. The time delay of the second stage cascode contributes to produce an output signal ($V_{out}^{(2)}$) with a peaking time of about 50 ns.

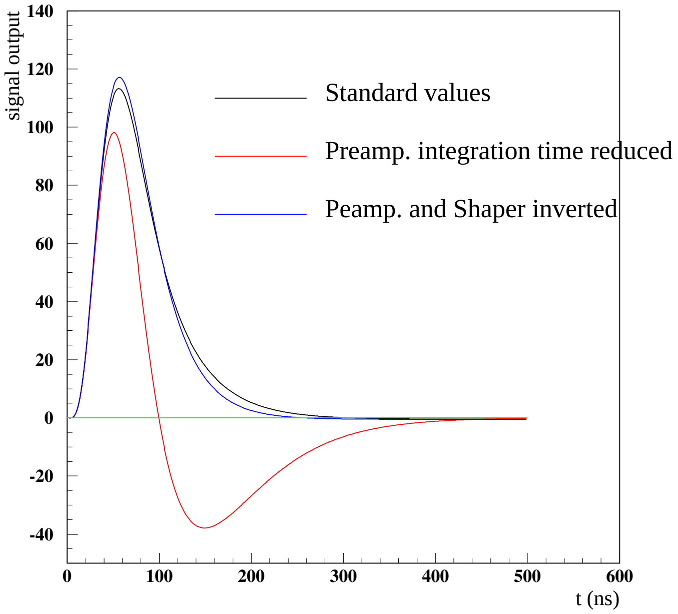

Figure 9: Prediction of the front-end channel model for different combination of the two stages time constants.

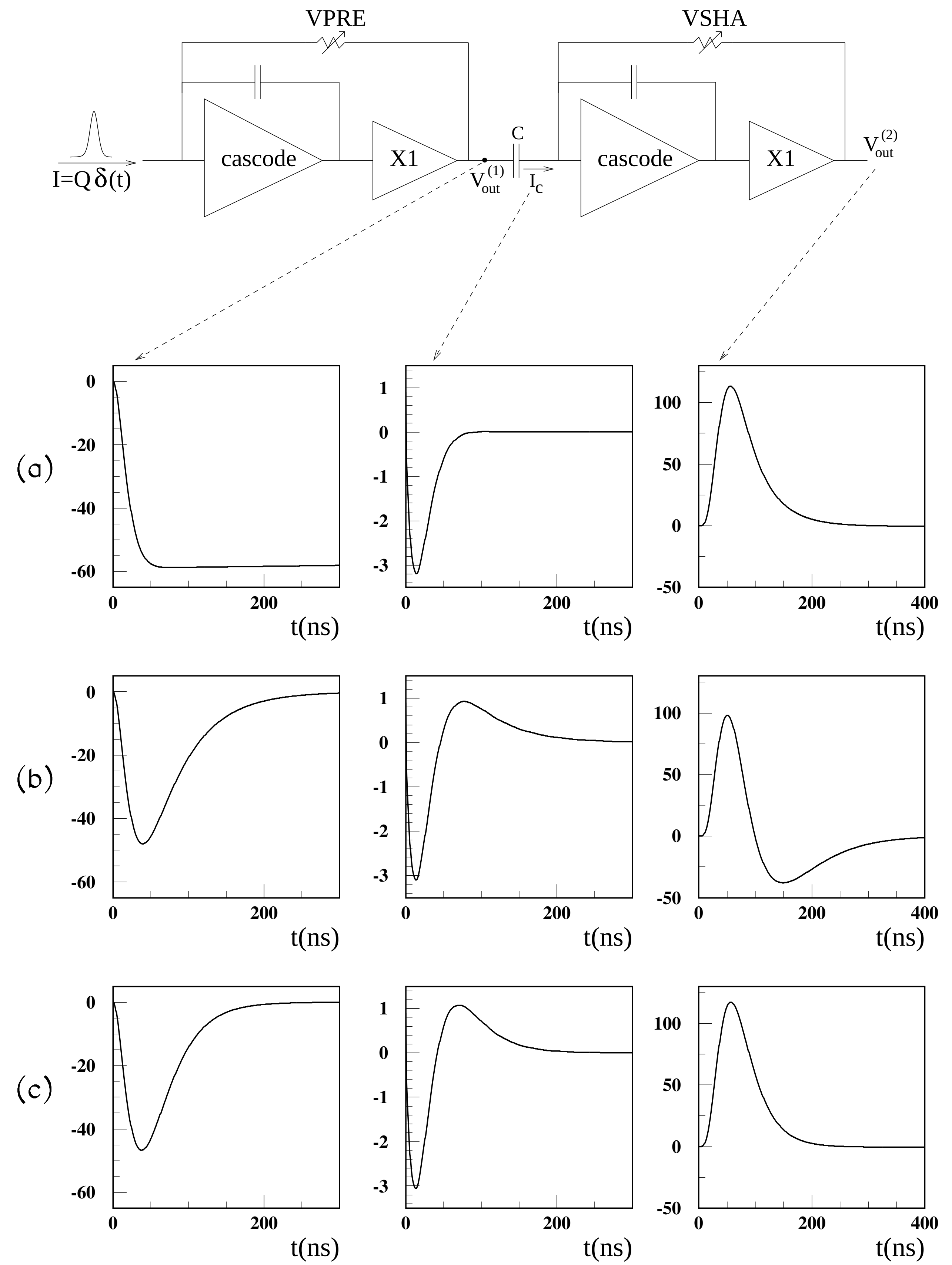

Figure 10: First stage voltage output ($V_{out}^{(1)}$), second stage current input (I_c) and voltage output ($V_{out}^{(2)}$) for three different combination of time constants:(a) standard time constants, (b) reduced time constant of the first stage, (c) inverted time constants of the two stages.

1.5 Further considerations on noise

It is interensting to investigate the possible raise of an additional noise related to the behaviour of the shaper output in high rate conditions, for standard settings of the APV6 chip registers (VSHA=0, VPRE=184).

Figure 11 (a) and (b) show respectively the output of preamplifier ($V_{out}^{(1)}$) and shaper ($V_{out}^{(2)}$) in the case of particles arriving with at the preamplifier input with constant time interval. All the input particles are simulated with the same height, normalized in order to have a shaper output of 40 in arbitrary units.

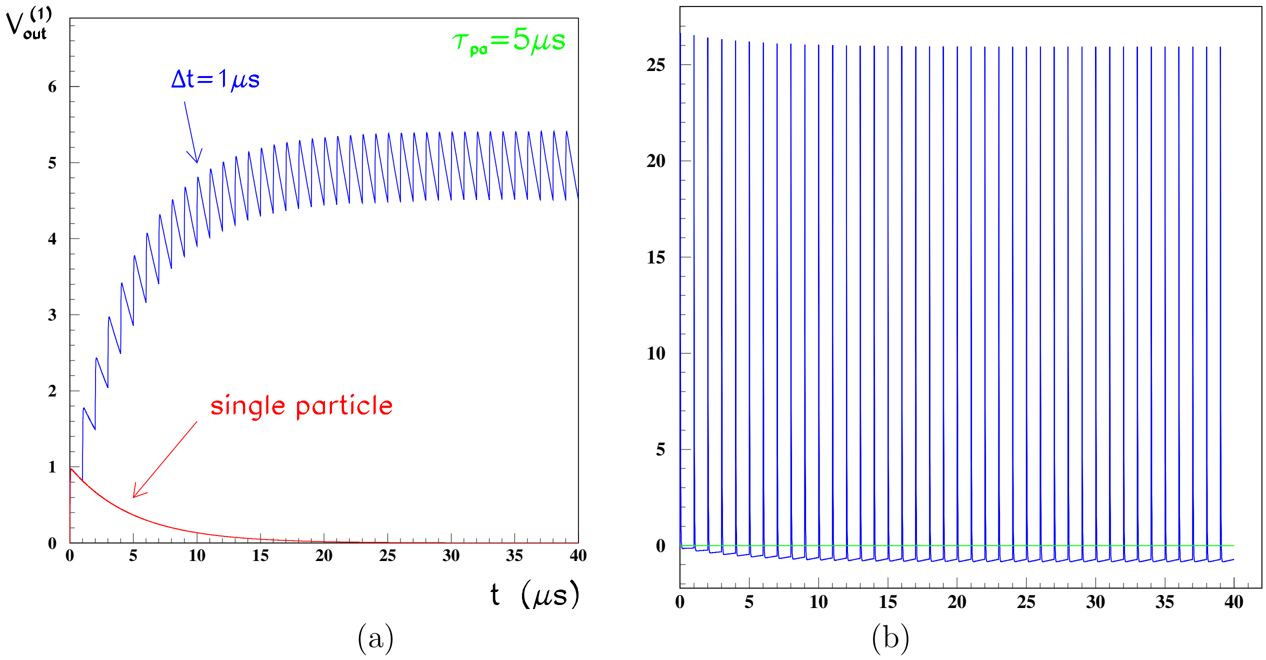

Figure 11: Preamplifier output (a) and shaper output (b) in arbitrary units for 1 MHz rate particles with a constant time interval distribution.

Figure 12 (a) and (b) show respectively the output of preamplifier and shaper in the case of particles arriving with at the preamplifier input with a time interval as expected at CMS (figure 13(a)). Input particles are simulated with a height distributed according to the Landau distribution (figure 13(b)) with a most probable value normilized in order to have a shaper output of 40 in arbitrary units.

It comes out that in the case of constant time interval the overall effect is a pedestal shift while in the case of actual time interval distribution there are also pedestal fluctuations added to the pedestal shift. Such fluctuations introduce a noise (figure 14) of the order of 1% of the Mip most probable value.

1.6 Conclusions

The results we obtained suggest that the VLSI front-end prototype planned for CMS silicon tracker can maintain its functionality at LHC high particle rates, if we work with small feedback time constant for the first stage and large feedback time constant for the second one. This method can be applied with any front-end chain which shows a complete symmetry between input and output stages.

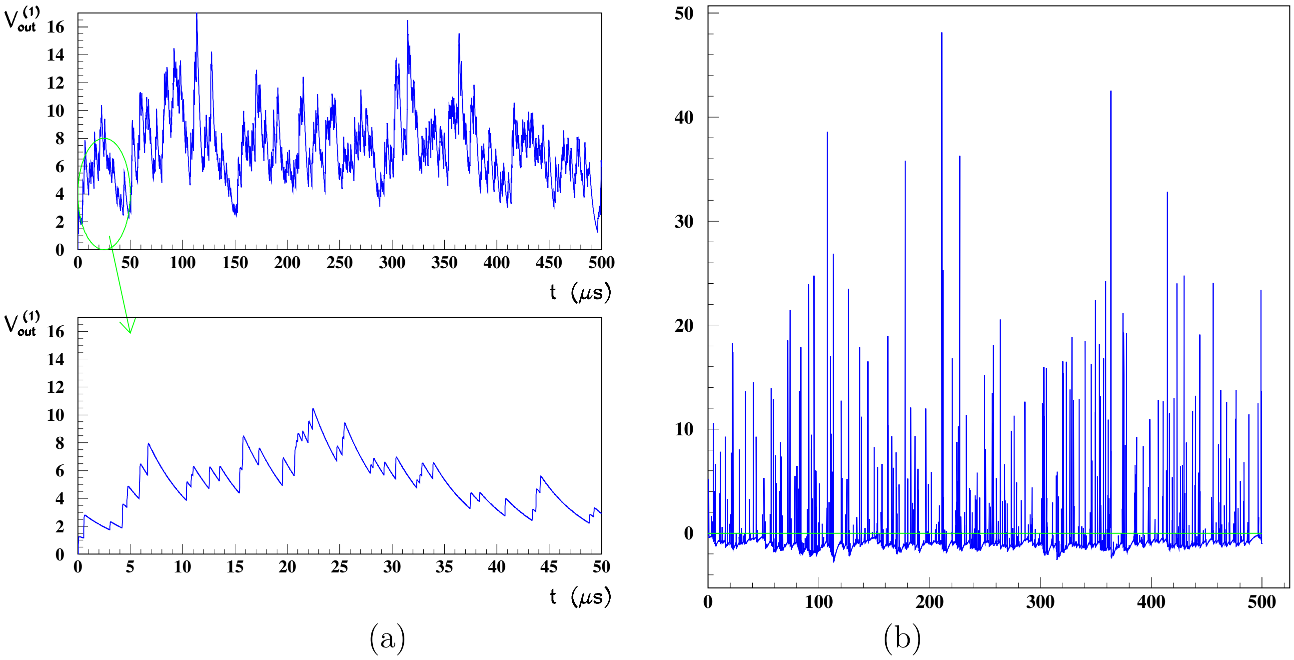

Figure 12: Preamplifier output (a) and shaper output (b) in arbitrary units for 1 MHz rate particles with a time interval distribution as expected at CMS (figure 13 (a)).

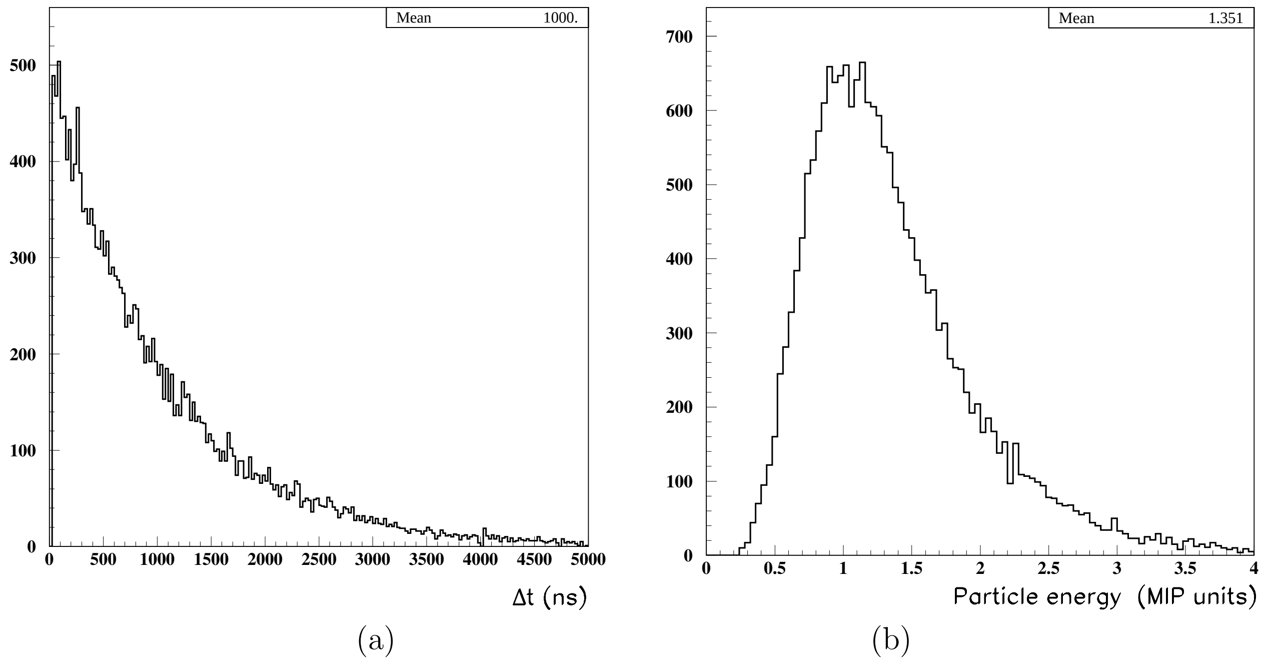

Figure 13: Time interval distribution (a) and energy distribution (b) of simulated particles arriving at the input preamplifier.

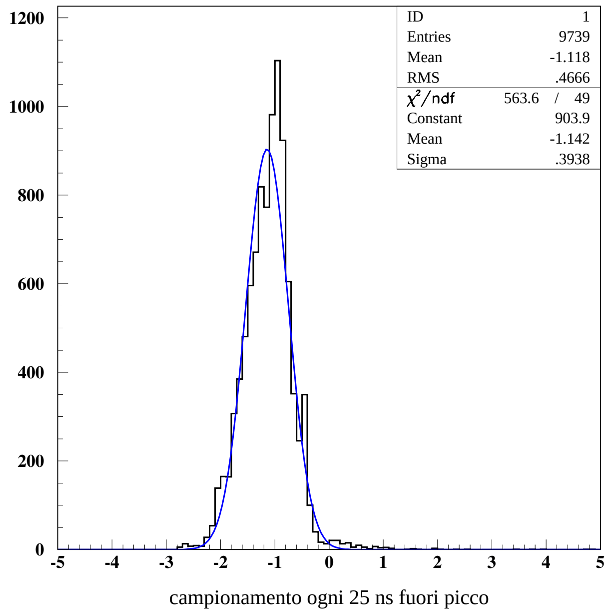

Figure 14: Noise (arbitrary units) coming from the output fluctuations related to the chip response to random arrival of particles at 1 MHz rate.